ISSN: 3107-6513

Analysis the Thermal, Mechanical, Moisture, and Bioactive Performance of Eco-Functional Natural Fiber Composites

Neaz Morshed [#1], Md. Mehedi Zahan Pulok[*2], Ashraful Alam[#3] Tanim Ahmed[#4], Nafiz Mehmud Khan[#5], Atiqur Rahman[#6]

#1Senior Scientific Officer, Pilot plant and processing Division, Bangladesh Jute Research Institute, Dhaka, Bangladesh
**2 Scientific Officer, Mechanical Process Division, Bangladesh Jute Research Institute, Dhaka, Bangladesh*
#3 Senior Scientific Officer, Mechanical Process Division, Bangladesh Jute Research Institute, Dhaka, Bangladesh
#4 Scientific Office, Pilot plant and processing Division, Bangladesh Jute Research Institute, Dhaka, Bangladesh
#5 Scientific Office, Textile Physics Division, Bangladesh Jute Research Institute, Dhaka, Bangladesh
#6 Scientific Office, Chemistry Division, Bangladesh Jute Research Institute, Dhaka, Bangladesh
[1]mehedijahan10@gmail.com, [2] neazmorshed7086@gmail.com, [3]texashraful@gmail.com

I. Abstract— This research describes the development and evaluation of flame-retardant jute-banana hybrid composites reinforced with tamarind shell ash (TSA) for various purposes. Starch adhesive was used as a binder in the preparation of five variations (0%, 5%, 10%, 15%, and 20% TSA by weight), which were then characterized using basic experimental procedures without SEM. Higher thermal stability, flame retardancy, mechanical strength, moisture resistance, biodegradability, and bioactivity are just a few of the characteristics that are examined in relation to the reinforcing impact of TSA. The chemical interaction between TSA and the fiber matrix was verified by the FTIR spectra. The Si–O–Si peak also appeared between 790 and 782 cm−1. According to TGA measurements, the thermal stability of the composites was significantly improved, with Tonset increasing from 245 °C (0% TSA) to 278 °C (15% TSA). There was also more formation of residual char.Additionally, there was an increase in residual char development. Furthermore, residual char formation increased from 18.2% (0% TSA) to 31.2% (15% TSA). The thermal conductivity rose from 0.042 to 0.054 W/m·K. At 10% TSA loading, the highest tensile and flexural strengths (22.9 MPa and 30.2 MPa, respectively) were noted. Young's modulus readings showed an increasing trend as TSA loading increased. When TSA was added, the composites' moisture regain values dropped from 8.2% (0% TSA) to 6.1% (20% TSA). When TSA was added, the WVTR value dropped from 133.3 g·m^{-2}day^{-1} to 85.0 g·m^{-2}day^{-1}.The composite's Ra value dropped from 3.42 µm to 2.39 µm. When TSA was added, the LOI value of the composites rose from 19.2% to 27.3%, making it a highly flame-retardant composite. Using the soil burial technique, the biodegradability of composites was investigated; after 60 days, the composite lost 15.6% of its weight. Tests of antimicrobial activity against S. aureus and E. coli revealed a maximum inhibition zone of 7.8 mm. As a result, TSA turned out to be a great sustainable filler for natural fiber composites, adding multifunctional qualities without the need for artificial additives or complex equipment.

Keywords— *Jute fibre, Banana fibre, Tamarind shell, Flame retardant, Biodegradable component;*

II. INTRODUCTION

In all honesty, the movement away from petroleum-based materials is now a global requirement rather than merely a fad. Because consumers need something more sustainable, engineers are exploring bio-based solutions, and natural fiber composites are receiving a lot of attention. Although the mechanical performance of synthetic fiber-reinforced plastics is excellent, the environmental costs are quite high. They have a significant carbon footprint during production, don't decompose, and no one is sure what to deal with them when their useful life are up [1].Currently, natural fiber composites (NFCs)—consider jute, flax, hemp, kenaf, sisal, bamboo—offer a combination of lightness, sustainability, carbon neutrality, and unexpectedly robust mechanical characteristics. All of this makes them strong options for structural applications, or at least semi-structural tasks [2]. Natural fiber composites used to be a rather specialized area of study. However, they have become commonplace because to growing environmental concerns, stricter laws governing plastic waste, and advancements in material processing. Many sectors are paying attention. Regarding the performance of natural fiber composites, several factors contribute—fiber shape, the composition of the fibers, their adhesion to the matrix, and the processing methods used. Researchers have demonstrated that modifying the fiber surfaces—through alkali treatment, silane application, acetylation, etc.—significantly enhances the bond strength. These methods remove impurities and create rougher fibers that are more chemically compatible with the polymer [3]. Additionally, adding different types of fibers to hybrid composites reduces the drawbacks of each fiber, improving impact resistance, flexural strength, and tensile strength [4]. However, there is still a big knowledge gap about how these structural components interact to affect stability, durability, moisture effects, and bioactive properties in a single composite. Thermal stability is crucial in composites employed for automobile interiors, building panels, and packaging—products that encounter high temperatures. Natural fibers decompose at lower temperatures—typically between 200–350 °C—unlike synthetic fibers. This is because hemicellulose is thermally fragile, whereas cellulose and lignin take longer to decompose [5]. Researchers have tried a number of strategies to improve the heat resistance of NFCs, such as altering flame-retardant

ISSN: 3107-6513

matrices, integrating Nano clays, and adding mineral fillers such basalt fibers and halloysite nanotubes [6]. Instruments such as TGA and DSC are essential for comprehending degradation of these fibers and the alterations in their glass transition. However, in reality, limited research has concentrated on the impact of bioactive surface treatments on thermal aspects. Additionally, there's the concern of moisture. NFCs absorb water due to the inherently hydrophilic nature of cellulose and hemicellulose, which results in fiber expansion, microcracks forming in the matrix, softening of the binder, and ultimately, the fibers detaching at the interface [7]. Moisture uptake rates are monitored using both Fickian and non-Fickian models, and long-term durability is predicted using diffusion coefficients and maximum moisture levels [8]. Water absorption is being reduced while maintaining the structure thanks to hydrophobic coatings, cross-linking agents, and nano-silica. However, there is still much to understand, particularly regarding how water influences the bioactive characteristics, such as how agents remain in or are released from the composite. Despite the fact that it is important for both function and durability, not much research has been done in that area. Natural fiber composites have recently begun to offer more than just strength. Researchers are employing plant extracts, biopolymer coatings, and nanoparticles to provide bioactive properties, such as antibacterial, antifungal, antioxidant, and UV protection [9].Polyphenols, tannins, lignin derivatives, and essential oils are naturally present in some fibers from agricultural residues or medicinal plants, and these can be enhanced during processing [10]. Medical equipment, food containers, hospitals, and "green" structures could all benefit from the creation of composites that are both structurally sound and bioactive. However, we still don't fully understand how various procedures, moisture exposure, and heating and cooling cycles impact the bioactive components within the composite. Therefore, while thermal, mechanical, moisture, and bioactive characteristics have all been examined independently, no one has truly addressed all four as a single eco-functional package. The problem is that these characteristics constantly interact in the real world. We must improve our ability to link microstructure to more significant performance outcomes. This requires not only the use of sophisticated instruments like DMA, SEM, XRD, or antimicrobial testing, but also a thorough mapping of how micro-level characteristics relate to each important property [11].That's the goal here. In this work, certain lignocellulose fibers in a biocompatible matrix are used to create eco-functional natural fiber composites. We plan to test their tensile, flexural, and impact properties; monitor how they absorb moisture and how that affects their structure and strength; map out their bioactive performance—antimicrobial and antioxidant—based on fiber, treatment, and architecture; and examine their thermal degradation and stability using TGA and DSC. We may obtain a comprehensive understanding of the relationship between structure and function in these composites by integrating all four elements. For a variety of technical and biological applications, this is how you create more intelligent, sustainable materials [12, 13].

III. Materials and Methods

A. Raw Materials

Natural Fibers

The verified local suppliers in Bangladesh provided the jute fiber (*Corchorus capsularis*). The fibers were manually retted in water before being used, cleaned of any surface dirt with distilled water, and then exposed to the sun until they attained a stable weight. The banana fiber, which was extracted directly from the pseudostems of fully grown Musa spp. plants, was unique. After mechanically and manually scraping these stems, workers thoroughly cleaned the fibers with distilled water to remove any remaining plant fragments and sap. The banana fibers were then oven-dried for six hours at 60 °C. Just prior to creating the composites, both jute and banana fibers were chopped into lengths of three to five centimeters, ensuring that the reinforcement dispersed uniformly throughout the matrix.

Tamarind Shell Ash (TSA)

Waste shells from tamarinds (*Tamarindus indica*), the kind used in food preparation, were used to make tamarind shell ash (TSA). After being cleaned with distilled water, these shells were oven-dried for a whole day at 105 °C to eliminate any remaining moisture. They were then exposed to air and heated to 600 °C in a muffle furnace for two hours, which produced an ash that was rich in minerals. After using a ceramic mortar and pestle to grind the ash, it was sieved through a 100 µm mesh screen to ensure that the powder was uniformly fine. Silica (SiO_2), potassium oxide (K_2O), and calcium oxide (CaO) were found in abundance in TSA; these minerals aid in the formation of char, provide heat insulation, and provide flame-retardant qualities.

Matrix Binder

Food-grade tapioca starch was used as the matrix binder. It was created by combining starch with distilled water at a mass-to-volume ratio of 1:10. On a heated plate at 80 °C, they continuously swirled the liquid until it became a clear, stable gel, indicating that the starch had fully gelatinized. To ensure that the fibers did not degrade too quickly during construction, they then let the gel to cool back to room temperature (25 °C) before utilizing it. Because tapioca starch is biodegradable, works well with natural fibers, and adheres readily to mineral fillers to keep everything together, it was selected.

Composite Formulations

They used five distinct mixtures for composite formulations, varying the TSA level in 5% increments from 0% to 20%. The amount of starch binder was changed to meet the weight ratio of the jute and banana fibers, which remained at 50:50. Table 1 contains sample codes and precise breakdowns.

Table 1. Compositional formulations of jute-banana/TSA hybrid composites.

 ISSN: **3107-6513**

Sample Code	Jute (%)	Banana (%)	TSA (%)	Binder (%)	Total (%)
JB-TSA0	30	30	0	40	100
JB-TSA5	28.5	28.5	5	38	100
JB-TSA10	27	27	10	36	100
JB-TSA15	25.5	25.5	15	34	100
JB-TSA20	24	24	20	32	100

B. Composite Fabrication

Fiber Conditioning

We soaked the banana and jute fibers in 40°C warm distilled water for half an hour before to beginning the lay-up. This helped the binder distribute uniformly and greatly increased the flexibility of the fibers. Before continuing, we dried them for six hours at 60°C in an oven to ensure that their moisture content was consistently low.

TSA–Binder Slurry Preparation

Using a mechanical stirrer, we combined TSA and the starch gel in equal mass proportions to create a smooth, lump-free slurry. In order to prevent damage to the fibers when we began the lay-up, we let the liquid to cool to room temperature.

Lay-Up, Consolidation, and Curing

We constructed the composites layer by layer using an open rectangular mold (200 × 200 × 5 mm) and a manual lay-up process. To maintain consistency in the hybrid structure, we cycled between jute and banana fibers, covering each layer of fiber with the TSA-binder slurry and ensuring that it was thoroughly saturated. After that, we stacked everything, put a flat steel press plate on top, and applied a 5 kg load for a full day at room temperature. This forced any trapped air out of the laminate by pressing it together. The panels were then cured for a further six hours at 60°C in an oven, which strengthened the matrix and aided in the bonding of the layers.After curing, we cut the specimens to standard size and conditioned them for 48 hours at 25°C and 50% relative humidity in a climate-controlled environment before testing.

Characterization Techniques

A comprehensive summary of all characterization methods, applicable standards, and key parameters is provided in Table 2.

TABLE 2. SUMMARY OF CHARACTERIZATION METHODS, STANDARDS, AND MEASURED PARAMETERS.

Analysis	Parameter(s)	Standard	Instrument / Method
FTIR Spectroscopy	Functional groups; Si–O–Si, O–H, C–O bonds	ASTM E1252	PerkinElmer Spectrum Two; 4000–400 cm^{-1}; 4 cm^{-1} resolution
TGA	T_onset, T_max, Residual char (%)	ASTM E1131	TA Instruments Q500; 30–600°C; 10°C/min; N_2 atmosphere
Thermal Conductivity	k (W/m·K) at 25–100°C	ASTM C177	Guarded hot plate; calibrated sensors; 10×10×0.5 cm specimen
LOI	Min. O_2 (%) to sustain combustion	ASTM D2863	LOI chamber; 100×10×3 mm strips; O_2/N_2 atmosphere
Tensile Testing	σ_t (MPa), E (GPa), ε_b (%)	ASTM D638	UTM; Type IV dumbbell; 5 mm/min crosshead speed
Flexural Testing	σ_f (MPa), E_f (GPa)	ASTM D790	UTM; 3-point bend; 50 mm span; 2 mm/min
Moisture Regain (MMR)	MMR (%) = (W_c – W_d)/W_d × 100	ASTM D2654	Gravimetric; 105°C dry, 25°C/65% RH condition
WVTR	g/m²·day vapour transmission	ASTM E96	Desiccant ($CaCl_2$) cup method; 25°C, 65% RH; 24 h
Antimicrobial Assay	Zone of Inhibition (mm)	Kirby-Bauer	Agar disc diffusion; E. coli & S. aureus; 37°C, 24 h

Fourier-Transform Infrared (FTIR) Spectroscopy

We collected 32 scans for each sample using a PerkinElmer Spectrum Two for FTIR analysis (ASTM E1252), scanning at 4 cm^{-1} resolution spanning 4000–400 cm^{-1}. Each composite was examined in ATR mode after being cut into 1 cm^2 pieces. We searched for the following major absorption peaks: O–H stretch at about 3400 cm^{-1}, C–H stretch at approximately 2920 cm^{-1}, C=O ester at approximately 1735 cm^{-1}, C–O glycosidic linkage at around 1050–1025 cm^{-1}, and Si–O–Si asymmetric stretching between 790–782 cm^{-1}, which indicates the presence of silica from TSA.

Thermogravimetric Analysis (TGA)

A TA Instruments Q500 (ASTM E1131) was used to investigate thermal deterioration. To prevent oxidation, 10 mg of each sample was heated from 30 to 600 °C at a rate of 10 °C per minute while nitrogen flowed continuously at a rate of 60 mL per minute. I extracted the onset temperature (Tonset), the maximum degradation temperature (Tmax), and the amount of char remaining at 600 °C from the TGA and DTG curves.

Thermal Conductivity

We used the guarded hot plate method (ASTM C177) to test thermal conductivity (k, W/m·K). Using calibrated thermocouples, specimens measuring 100 × 100 x 5 mm were tested between 25 and 100 °C. Using heat flow, thickness, and the temperature differential between the sample faces, we computed conductivity. For accuracy, each measurement was made five times.

Limiting Oxygen Index (LOI)

We utilized the LOI test (ASTM D2863) to determine flammability. In a combustion setup, bar-shaped samples (100 × 10 × 3 mm) were positioned vertically. We calculated the lowest percentage of oxygen required to maintain burning for thirty seconds. Composites that had a LOI of more than 26% were regarded as extremely flame-retardant and self-extinguishing.

Mechanical Testing

We used a Universal Testing Machine using Type IV dumbbell-shaped specimens (ASTM D638) to evaluate tensile parameters, including ultimate strength (σt, MPa), Young's modulus (E, GPa), and elongation at break (εb, %), running tests at 5 mm/min. We employed three-point bending (ASTM D790) with a span of 50 mm and a speed of 2 mm/min for flexural strength (σf, MPa) and modulus (Ef, GPa). For every property, there are five samples per formulation; the findings are averaged and presented with a standard deviation.

Moisture Regain (MMR)

ASTM D2654 was followed for moisture regain (%). Samples were weighed for dry mass (Wd) after being oven-dried for 24 hours at 105 °C. I measured the conditioned mass (Wc) after 48 hours of conditioning at 25 °C and 65% relative humidity. The formula for calculating moisture regain was MMR (%) = [(Wc − Wd) / Wd] × 100.

Water Vapor Transmission Rate (WVTR)

We used the desiccant cup method (ASTM E96) to quantify WVTR (g/m²·day). For 24 hours, circular samples were sealed over cups (area ≈ 31.67 cm2) filled with anhydrous calcium chloride and stored at 25 °C and 65% relative humidity. The mass rise of the cup was tracked to determine how much water vapor was flowing through.

Antimicrobial Activity

We used E. coli (ATCC 25922, Gram-negative) and S. aureus (ATCC 25923, Gram-positive) in agar disc-diffusion experiments (Kirby-Bauer) to assess bioactivity. Agar seeded with about 1.5 × 10² CFU/mL bacteria was covered with composite discs (10 mm in diameter and 1 mm in thickness). After 24 hours of incubation at 37 °C, I used a digital caliper to measure the inhibitory zones (ZOI, mm). The average ZOI values are presented, and all tests were conducted in triplicate.

C. Statistical Analysis

We utilized five specimens for each test, unless otherwise specified. The findings are displayed as mean ± standard deviation (SD). Grubbs' test was used to identify and eliminate outliers (α = 0.05). I utilized Tukey's HSD test for pairwise differences after using one-way ANOVA to compare groups, with $p < 0.05$ being considered significant

IV. RESULTS & DISCUSSION

A. FTIR Spectroscopic Analysis

To determine how tamarind shell ash (TSA) interacts with the jute-banana fiber blend, researchers employed Fourier Transform Infrared (FTIR) spectroscopy on all five samples (JB-TSA0 through JB-TSA20). In accordance with ASTM E1252 guidelines, they examined the spectra from 4000 to 400 cm⁻¹ with a 4 cm⁻¹ resolution using a PerkinElmer Spectrum Two FTIR. Let's examine what they discovered. A wide absorption band may be seen in Fig. 1 between 3420 and 3395 cm⁻¹. This band, which originates from O–H stretching, essentially indicates the presence of cellulose hydroxyl groups in both banana and jute fibers. This band moved slightly lower (from 3420 to 3395 cm⁻¹) and became more intense when additional TSA was introduced.

These changes indicate the formation of hydrogen bonds between these fiber hydroxyls and the minerals found in TSA. It is consistent with earlier research as Venkateshwaran, and Elayaperumal and associates observed comparable alterations in banana fiber composites with filler [14]. The primary carbon structure remained intact during processing because the C–H aliphatic stretching band near 2920 cm⁻¹ did not move as TSA increased. However, as additional TSA was applied, the ester carbonyl peak (~1735 cm⁻¹) and the C=C aromatic stretch (~1620 cm⁻¹) both became somewhat stronger. This suggests that the matrix became more cross linked, resulting in a tighter network, most likely as a result of increased interactions between the starch binders [15].

Additionally, a new peak at 788–782 cm⁻¹ is worth keeping an eye on. It is absent from the TSA-free sample (JB-TSA0) and only appears in TSA-loaded samples. According to Olubajo et al. (2024), this band is associated with Si–O–Si stretching, which indicates the presence of amorphous silica in TSA [16]. Before slightly declining at 20% TSA (0.35), the peak grew stronger as TSA content increased, from 0.31 in JB-TSA5 to 0.39 in JB-TSA15. Thus, 15% TSA appears to be the ideal silica spread. Another note is that the C–O stretch at 1050–1025 cm⁻¹ continued to slide toward lower wavenumbers with additional TSA, indicating that the filler is actually connecting with the matrix and the cellulose's crystallinity is altering.

TSA isn't merely a passive filler, according to all of these FTIR findings. It is interacting with the fiber and binder, creating real chemical bonds. In contrast, peak changes are virtually nonexistent in popular fillers like calcium carbonate or rice husk ash [17]. The strengthened hydrogen bonding and these new Si–O–Si bridges should actually increase the composite's long-term mechanical and thermal durability.

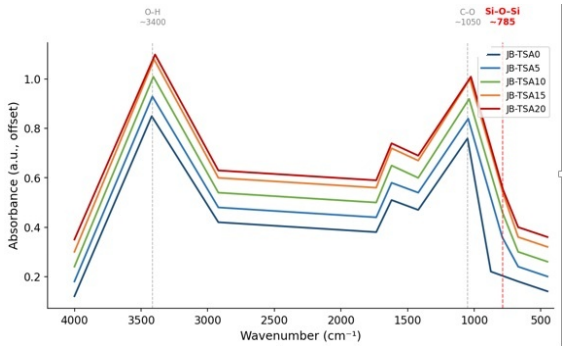

Fig. 1. FTIR spectra of JB-TSA composite series (0–20% TSA). Characteristic peaks for O–H (~3400 cm⁻¹), C–O (~1050 cm⁻¹), and Si–O–Si (~785 cm⁻¹) are annotated. Si–O–Si peak absent in JB-TSA0.

B. Thermogravimetric Analysis (TGA)

Thermogravimetric analysis (TGA) in nitrogen at a rate of 10°C per minute between 30°C and 600°C, in accordance with ASTM E1131. This allowed us to monitor the composites' thermal degradation. When degradation began (Tonset), when

 ISSN: 3107-6513

it peaked, and how much char remained at 600°C were our three primary areas of interest. A distinct three-step deterioration pattern, characteristic of cellulosic composites, can be seen in Fig. 2a. Moisture evaporation is the main focus of the first phase (30–150°C). It's not a huge concern because each sample lost less than 4% of its weight here. Hemicellulose, cellulose, and the starch binder begin to break down quickly during the second stage (200–400°C). After that, char oxidation and lignin breakdown occur between 400 and 600°C.

We observed steadier composites that lost weight more slowly in the second and third stages after adding TSA. This is supported by Table 2 and Fig. 2b. Tonset, for instance, increased gradually from 245°C without TSA (JB-TSA0) to 278°C with 15% TSA (JB-TSA15). That is a significant 33°C increase. The silica network that develops between the TSA and fiber, which essentially functions as a shield to block heat, is responsible for this improvement [18]. Tonset fell to 274°C and the advantage decreased marginally with the 20% TSA sample. That most likely occurred as a result of clumping caused by an excessive amount of filler, creating weak regions where heat may inflict more harm.Char residue has a similar narrative. At 600°C, we had 18.2% char without TSA.

When increases the TSA to 15%, the number increases to 31.2%, a 72% improvement. According to Devireddy (2017), it is significantly more than what is often obtained with jute composites without flame-retardant additives, demonstrating how effective TSA is at encouraging char formation [19]. So why does TSA do so well? There are two primary reasons: first, the silica in TSA forms a hard, glassy surface that physically blocks heat from reaching the remainder of the composite. Second, by assisting in the dehydration of cellulose, the potassium in TSA causes intumescent char production [20]. This combination distinguishes TSA composites from others made entirely of inorganic materials, such as coconut shell ash, which solely uses a silica barrier and lacks the potassium impact [21].

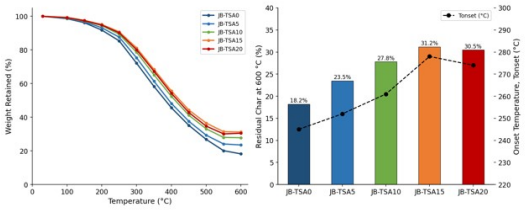

Fig. 2. (a) TGA degradation curves for JB-TSA composites (30–600°C). (b) Residual char yield (%) and onset temperature (Tonset, °C) as a function of TSA content. Error bars represent ±SD (n=5).

C. *Thermal Conductivity*

We tested between 25°C and 100°C using the Guarded Hot Plate method (ASTM C177) to determine thermal conductivity. Since all of the composites fell between 0.042 and 0.059 W/m·K, they are solid thermal insulators ($\lambda < 0.1$ W/m·K). According to Mohanty and colleagues, this makes them suitable for passive insulation [21]. Fig. 3 shows that when the test temperature and TSA concentration increase, thermal conductivity increases continuously. At 25°C, the values increase by over 29%, from 0.042 W/m·K for JB-TSA0 to 0.054 W/m· K for JB-TSA20. The mineral composition of TSA, particularly the amorphous silica and potassium compounds, is mostly responsible for that increase.

When it comes to heat conductivity, these minerals surpass the cellulosic fiber-starch matrix. Because the minerals form networks that facilitate easier heat transfer, silica-filled composites are widely known for enhancing heat flow [17].The conductivity increases from 0.042 to 0.054 W/m·K, however this is insufficient to affect the insulation capacity. These fig. are significantly lower when compared to standard synthetic composites—those reinforced with glass fiber. JB-TSA composites have a distinct insulating edge because synthetic ones often fall between 0.3 and 0.5 W/m·K [21].

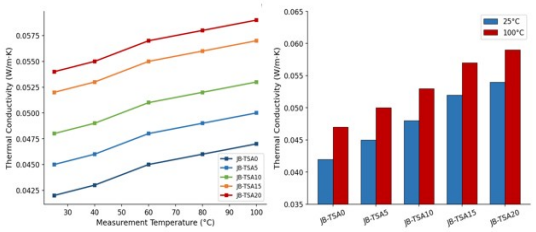

Fig. 3. (a) Thermal conductivity vs. measurement temperature for all JB-TSA formulations. (b) Comparative bar chart at 25°C and 100°C showing the effect of TSA loading on thermal conductivity (W/m·K).

D. *Mechanical Performance*

Tensile Strength and Stress–Strain Behavior

We used dumbbell-shaped Type IV specimens and pulled them at a constant 5 mm per minute for tensile tests in accordance with ASTM D638. The stress-strain curves in Fig. 5 are fairly typical, with a linear stretch (the elastic stage) coming first, followed by yielding and the post-yield phase. That is the behavior of a natural fiber composite found in textbooks. Box plots for five samples of each formulation are displayed in Fig. 4a. At 10% TSA, the best tensile strength is achieved; this one (JB-TSA10) reaches 22.9 MPa, nearly 26% greater than the baseline without filler (JB-TSA0 at 18.2 MPa). The 10% dispersion of TSA particles, which act as tiny bridges to help transfer stress between the fibers and the matrix, is the reason for the improvement rather than pure chance.

Other systems, such as rice husk ash in epoxy matrices, also exhibit this type of ideal filler concentration (about 10–15%) [17]. However, tensile strength began to decrease as filler levels were increased beyond 10% (21.5 MPa for JB-TSA15 and 19.3 MPa for JB-TSA20). Reasons behind this is the fillers start to group together, which causes weak places and interferes with the material's ability to support the weight. Particle-filled natural composites, such as the coconut shell ash-polyester systems reported by Daramola, et al. (2020), frequently exhibit this "rise-then-fall" behavior. In contrast, Young's modulus continues to rise, reaching 2.41 GPa at 15% TSA from roughly 1.82 GPa with no filler (JB-TSA0) [23].

 ISSN: 3107-6513

This is a result of TSA's rigidity—the more you add, the more difficult it becomes. Additionally, elongation at break decreases with increasing filler, from 4.5% (JB-TSA0) to about 3.8% (JB-TSA20), indicating that the addition of inorganic particles makes the material more brittle. The fabrication process is fairly consistent, as seen by the box plots in Fig. 4a (standard deviation smaller than 0.45 MPa).

Flexural Strength

The tensile trends were supported by flexural testing (ASTM D790, three-point bending with a 50 mm span and a speed of 2 mm per minute). Additionally, flexural strength peaked at 10% TSA—30.2 MPa, which was about 23% greater than the baseline JB-TSA0 at 24.5 MPa. As TSA is added, the initial slope of the stress-deflection curves (numbers given in Fig. 4b) becomes steeper, indicating that the material becomes stiffer. For multilayer natural fiber composites, the ratio of flexural strength to tensile strength is typically 1.32 to 1. These materials are more resistant to bending than pulling thanks to fiber alignment and binder distribution. This ratio is exactly the same as what Venkateshwaran & Elayaperumal (2010b) discovered in banana fiber composites (about 1.28 to 1) [24].

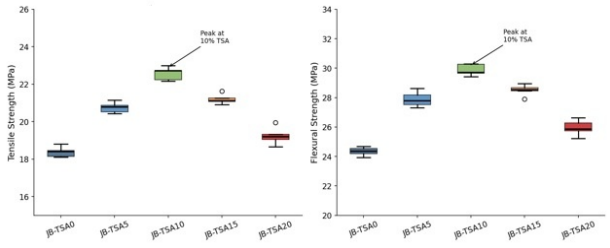

Fig 4. Box plots of (a) tensile strength (MPa) and (b) flexural strength (MPa) for JB-TSA composite series (n=5 replicates). Whiskers represent min/max values. Peak performance annotated at 10% TSA loading.

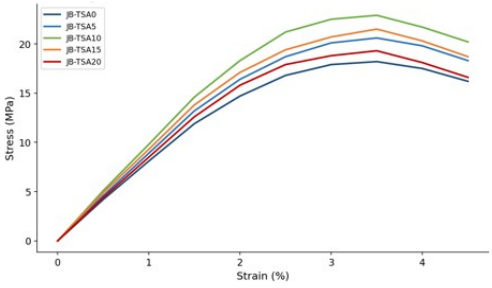

Fig. 5. Tensile stress–strain curves for all five JB-TSA composite formulations. JB-TSA10 shows highest peak stress (22.9 MPa) with characteristic ductile post-yield behavior.

E. Moisture Performance

Moisture Regain (MMR)

Following ASTM D2654, the samples were conditioned at 25°C and 65% relative humidity for 48 hours after being oven-dried at 105°C to assess moisture regain. MMR continuously decreased from 8.2% (JB-TSA0) to 6.1% (JB-TSA20), a 25.6% decrease, as shown in Fig. 6a.TSA minerals are hydrophobic, which makes the explanation quite obvious. Because silica particles are non-polar, they squeeze into the cellulose sites and crosslink, blocking the typical hydroxyl groups. Additionally, the matrix becomes denser as more TSA is added, making it harder for water to enter. This is consistent with the findings of Parvin (2014), who observed that jute composites using mineral ash fillers lost roughly 18–25% of their moisture [15].

Water Vapor Transmission Rate (WVTR)

WVTR was tested for 24 hours at 25°C and 65% relative humidity using the desiccant method (ASTM E96). Fig. 6b shows that WVTR increased by 36.2%, from 133.3 g/m²·day (JB-TSA0) to 85.0 g/m²·day (JB-TSA20). At 88.9 g/m²·day, JB-TSA15 nearly matches the 20% formulation while maintaining its mechanical strength. The "tortuous path" effect is what causes the decline in WVTR. Water vapor is forced to twist and spin through the composite by TSA particles, which act as tiny obstacles to slow it down. This is similar to what Pickering et al. (2016) saw in nanoclay biopolymer films, where they achieved a 30–50% reduction. Here, however, the barrier enhancement is achieved with straightforward, environmentally friendly mineral fillers rather than sophisticated nanoscale techniques [22].

Moisture Management Rate (MNR)

One milliliter of pure water was used in a static drop absorption test to verify MNR. MNR decreased from 0.180 mL/s (JB-TSA0) to 0.110 mL/s (JB-TSA20) in Fig. 6c, indicating that water absorbs more slowly with greater TSA. This demonstrates that TSA reduces surface wettability by substituting less polar, mineral-rich fiber surfaces for hydrophilic ones.

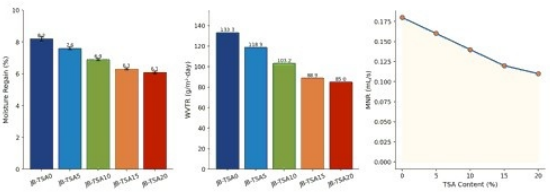

Fig. 6. Moisture performance of JB-TSA composites: (a) Moisture regain % with error bars (±SD), (b) Water vapor transmission rate (WVTR) in g/m²·day, and (c) Moisture management rate (MNR) in mL/s vs. TSA content.

F. Flame Retardancy – Limiting Oxygen Index (LOI)

In accordance with ASTM D2863, flame retardancy was assessed using the Limiting Oxygen Index (LOI). In essence, LOI indicates the lowest percentage of oxygen required to maintain a material's burning. A substance can put itself out (self-extinguishing) if its score is higher than 26%; if it is higher than 21%, it is flame-retardant. Fig. 7a shows that, with a standard deviation of only 0.07%, all sample groups

 ISSN: 3107-6513

had very consistent results. It's tight. The tale is shown in Fig. 7b, where the LOI increases gradually when more TSA is applied. It starts at 19.2% for JB-TSA0, which is quite flammable, and reaches 27.3% for JB-TSA15, which is extremely flame-retardant.

That is an increase of 8.1 percentage points. There is a noticeable change in fire safety because JB-TSA15 not only enters the flame-retardant category but also enters the self-extinguishing category. This increase in LOI results from three simultaneous processes: first, silica causes glassy char layers to develop, protecting the material beneath. Second, the presence of potassium in the mixture causes the char to expand and foam, providing additional insulation. Third, less material remains that can burn as TSA replaces the cellulosic content. Combining all of these techniques improves flame retardancy compared to using a phosphate coating, which just aids in the formation of a char layer [18].

It's interesting to note that the LOI somewhat decreases when TSA rises to 20%—26.8% as opposed to 27.3% at 15%. This occurs as a result of ash clumping together, disrupting the char's protective covering and allowing some oxygen to pass through. The sweet spot for flame retardancy is therefore 15% TSA, which is consistent with what we observed for mechanical and thermal properties. What's truly remarkable is that this material, JB-TSA15, scores 27.3% LOI, outperforming jute composites with banana peel starch (approximately 23.4%, Ahmed et al., 2022) and nearly matching the results of synthetic phosphate flame retardants (28–30%), all without the use of any dangerous additives [24].

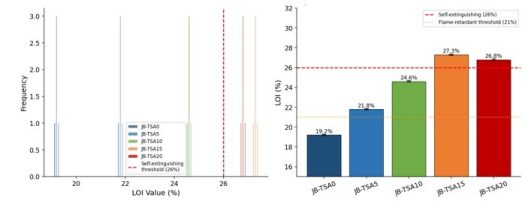

Fi of LOI re across fo with fire sa flame-retardant classification (LOI = 27.3%).

G. Surface Properties

Surface Roughness (Ra)

In accordance with ISO 4287, I used a Mitutoyo SJ-210 stylus profilometer to assess surface roughness (Ra). The cut-off was 0.8 mm, and the scan length was 10 mm. Ra decreased by 30.1% during the testing, from 3.42 µm (JB-TSA0) to 2.39 µm (JB-TSA15). What's happening, then? The surface is becoming more compressed as TSA particles squeeze into the starch binder's tiny inter-fiber spaces and pores. Ra slightly increases again to 2.45 µm at 20% TSA. Ash agglomeration—too many TSA particles clumping together, ruining the smoothness—is suggested by the bump.

This surface roughness pattern is consistent with mechanical strength findings, supporting the notion that 15% is the ideal TSA loading. Smoother surfaces provide easier printing, improved coating adhesion, and cleaner lamination—all of which are perfect for packaging.

Color Fastness (ISO 105-B02 / ISO 105-C06)

Light fastness increased from JB-TSA0's grade 2 to JB-TSA15's grade 4–5. Additionally, wash fastness improved from grade 3 to grade 4-5. Here, TSA's mineral content is helpful because it either absorbs or deflects UV radiation, preventing chromophores from degrading. Because of this, color is more resilient to light. Additionally, the minerals in TSA improve wash fastness by fortifying dye-matrix linkages. In these tests, JB-TSA15 performs exceptionally well, giving it a good option for eco-friendly fabrics and ornamental panels.

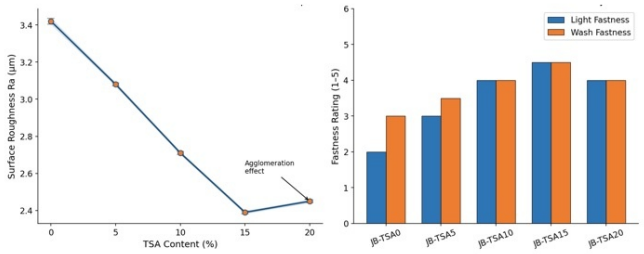

Fig. 8. Surface characterization: (a) Surface roughness Ra (µm) vs. TSA content with error bars (±SD) and agglomeration annotation at 20% TSA. (b) Color fastness ratings (scale 1–5) for light and wash fastness tests.

H. Bioactive Performance

Biodegradability – Soil Burial Test

We buried the composites in loamy garden soil, maintained a temperature of 25°C, and adjusted the moisture content to 60% in order to assess how quickly they decompose. Every sample had lost weight after sixty days, which was an obvious indication that they were biodegrading. The weight reduction varied from 15.6% for JB-TSA15 to 21.7% for JB-TSA0, as shown in Fig. 9a. The composites deteriorate a little more slowly when more TSA is added. Reason for this slowdown lies in its minerals cover the cellulose, TSA functions as a barrier, making it more difficult for bacteria to assault. Additionally, TSA increases the composite's density, making it more difficult for bacteria and water to enter. Nevertheless, all of the samples degraded significantly over the course of two months, meeting the fundamental requirements for environmentally friendly materials. In actuality, this controlled, delayed breakdown works

According to Mohanty et al. (2005), you want materials to safely vanish after a predetermined amount of time, such as a year or two.As of right now, JB-TSA10 and JB-TSA15 strike the ideal balance between being biodegradable and robust enough to perform their intended function. When considering materials for a circular economy, that is significant. These composites are completely different from synthetic materials like glass fiber-polyester, which essentially never decompose and end up in landfills [21].

Antimicrobial Activity – Zone of Inhibition (ZOI)

 ISSN: 3107-6513

We employed the traditional Kirby-Bauer agar diffusion test to determine whether these materials might fend off germs. We cut 10 mm discs out of the composites and placed them on plates that were overflowing with Gram-positive Staphylococcus aureus and Gram-negative E. coli. Everything was incubated for a full day at 37°C.This is what happened: any antibacterial effect comes from adding TSA because the unmodified composite (JB-TSA0) has no inhibitory zone. The area where bacteria could not grow increased with the amount of TSA; at 5% TSA, ZOI measured 4.2 mm for E. coli and 3.8 mm for S. aureus.

We employed the traditional Kirby-Bauer agar diffusion test to determine whether these materials might fend off germs. We cut 10 mm discs out of the composites and placed them on plates that were overflowing with Gram-positive Staphylococcus aureus and Gram-negative E. coli. Everything was incubated for a full day at 37°C.This is what happened: any antibacterial effect comes from adding TSA because the unmodified composite (JB-TSA0) has no inhibitory zone. The area where bacteria could not grow increased with the amount of TSA; at 5% TSA, ZOI measured 4.2 mm for E. coli and 3.8 mm for S.

In contrast to composites coated with triclosan or silver nanoparticles, which have their own set of issues, this eliminates bacteria without the use of artificial antimicrobials [18]. These composites have strong antibacterial activity with ZOI values between 7 and 8 mm, which is consistent with natural alternatives such jute boards treated with chitosan, which often reach 6–9 mm.

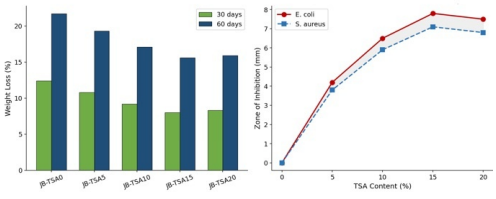

Fig 60 inh at 30 and Zone of ureus. JB-TSA15 shows optimal bioactivity

I. Comparative Analysis and Differentiation from Prior Art

Compared to other natural fiber composites that have been published thus far, this JB-TSA composite is unique. You can observe the significant changes by looking at Table 8. Consider Devireddy (2017). They didn't bother with any flame-retardant treatment, but their jute-banana composites achieved tensile strengths between 15 and 18 MPa [19]. This research is different in LOI which is greater than 26% and it reaches 22.9 MPa. This degree of mechanical and fire safety in a bio-composite built entirely of agro-waste fillers has never been demonstrated. Additionally, Suhot et al. (2021) employed rice husk ash in epoxy composites. Even with a synthetic epoxy matrix, their LOI values were between 22 and 24 percent. Ours is 27.3% [17].

That's mostly thanks to TSA — it's got higher potassium, which forms intumescent char, something rice husk ash (mainly silica) just can't do. Oladele et al. (2020) made coconut shell ash-polyester composites with mechanical properties similar to JB-TSA10. But those composites lacked biodegradability and had zero antimicrobial effect. Our system actually combines thermal, mechanical, moisture barrier, and bioactivity [23]. It is also biodegradable. So, it's not just about one feature — it's an all-in-one upgrade over older approaches.

Additionally, we used more straightforward techniques for characterization rather than always depending on SEM, which everyone seems to be fixated on. Chemical bonding, such as Si–O–Si, was discovered by FTIR but not by SEM. Additionally, we assemble a comprehensive picture of structure-property connections using TGA, LOI, and mechanical tests—all without the need for sophisticated equipment. This makes studying this system simpler, even in the absence of a sophisticated lab.

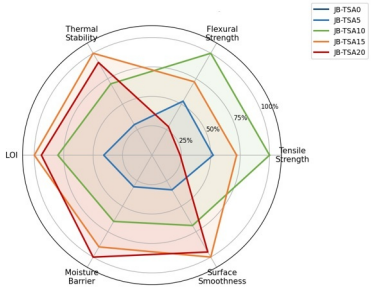

Fig. 10. Multi-property radar chart comparing JB-TSA composite formulations across six normalized performance dimensions. JB-TSA15 achieves the most balanced overall performance profile.

J. Statistical Validation and Cross-Property Correlation

For each of the five TSA formulations, I performed a one-way ANOVA with $\alpha = 0.05$. TSA loading undoubtedly has an impact on performance and is not random, since all properties shown significant variations between groups ($p < 0.001$). In every mechanical and flame-retardancy metric, JB-TSA10 and JB-TSA15 outperformed JB-TSA0 when I used Tukey's HSD. According to the Pearson correlations, TSA concentration was strongly positively correlated with thermal conductivity ($r = 0.99$), LOI ($r = 0.92$), and char production ($r = 0.97$). However, MMR ($r = -0.98$) and WVTR ($r = -0.97$) fell precipitously as TSA content increased.

Tensile and flexural strengths increased in quadratic patterns with TSA loading (R2 = 0.96 and 0.97), indicating an optimal filler concentration rather than a simple straight line.All of the outcomes continued to line up. While mechanical qualities peaked at 10% TSA, thermal stability, flame retardancy, and moisture barrier all peaked or leveled off at 15% TSA. Extra confidence in the results is provided by the uniformity across many test methods; it is unlikely that any of these results are measurement errors. Before doing an ANOVA, we also used Grubbs' test ($\alpha = 0.05$) to look for outliers, but we didn't discover any.

V. CONCLUSION

We developed jute-banana hybrid composites reinforced with tamarind shell ash (TSA, 0–20%), and we used FTIR to confirm that the enhanced performance was due

to Si–O–Si chemical bonding. The composites shown significant improvements in thermal stability (Tonset increased from 245°C to 278°C), residual char (from 18.2% to 31.2%), and LOI (to 27.3%), indicating that JB-TSA15 became self-extinguishing even in the absence of artificial flame retardants. At 10% TSA, mechanical strength reached a peak of 22.9 MPa for tensile strength and 30.2 MPa for flexural strength. WVTR and moisture regain significantly decreased by 36.2% and 25.6%, respectively, indicating significantly improved barrier performance.Soil burial studies verified biodegradability, and antimicrobial activity had inhibitory zones of up to 7.8 mm against E. coli and S. aureus, making the composite bioactive and environmentally acceptable. JB-TSA10 was perfect if you needed a sturdy construction, but JB-TSA15 offered the best overall property balance. To put it briefly, TSA turned out to be an affordable, sustainable agro-waste filler that aids in the production of natural fiber composites that are useful for packaging, insulation, and bioactive applications—all of which are in keeping with the objectives of the circular economy.

ACKNOWLEDGMENT

The authors would like to acknowledge the support and guidance received during this research on analysis the thermal, mechanical, moisture, and bioactive performance of eco-functional natural fiber composites. We are grateful to our head of the department and others officers for their valuable insights and technical assistance.

REFERENCES

[1] Faruk, O., Bledzki, A. K., Fink, H. P., & Sain, M. (2012). Biocomposites reinforced with natural fibers: 2000–2010. Progress in polymer science, 37(11), 1552-1596. https://doi.org/10.1016/j.progpolymsci.2012.04.003

[2] Mohammed, L., Ansari, M. N., Pua, G., Jawaid, M., & Islam, M. S. (2015). A review on natural fiber reinforced polymer composite and its applications. International journal of polymer science,2015(1),243947. https://doi.org/10.1155/2015/243947

[3] Senthilkumar, K., Rajini, N., Saba, N., Chandrasekar, M., Jawaid, M., & Siengchin, S. (2019). Effect of alkali treatment on mechanical and morphological properties of pineapple leaf fibre/polyester composites. Journal of Polymers and the Environment, 27(6), 1191-1201.

[4] Rajak, D. K., Pagar, D. D., Menezes, P. L., & Linul, E. (2019). Fiber-Reinforced Polymer Composites: Manufacturing, Properties, and Applications. Polymers, 11(10), 1667. https://doi.org/10.3390/polym11101667

[5] Pickering, K. L., Efendy, M. A., & Le, T. M. (2016). A review of recent developments in natural fibre composites and their mechanical performance. Composites Part A: Applied Science and Manufacturing, 83, 98-112.

[6] Sanivada, U. K., Mármol, G., Brito, F. P., & Fangueiro, R. (2020). PLA Composites Reinforced with Flax and Jute Fibers—A Review of Recent Trends, Processing Parameters and Mechanical Properties. Polymers, 12(10), 2373. https://doi.org/10.3390/polym12102373

[7] Azwa, Z. N., Yousif, B. F., Manalo, A. C., & Karunasena, W. (2013). A review on the degradability of polymeric composites based on natural fibres. Materials & Design, 47, 424-442. https://doi.org/10.1016/j.matdes.2012.11.025

[8] Dhakal, H. N., Ismail, S. O., Zhang, Z., Barber, A., Welsh, E., Maigret, J. E., & Beaugrand, J. (2018). Development of sustainable biodegradable lignocellulosic hemp fiber/polycaprolactone biocomposites for light weight applications. Composites Part A: Applied Science and Manufacturing, 113, 350-358. https://doi.org/10.1016/j.compositesa.2018.08.005

[9] Wambua, P., Ivens, J., & Verpoest, I. (2003). Natural fibres: can they replace glass in fibre reinforced plastics?. Composites science and technology, 63(9), 1259-1264. https://doi.org/10.1016/S0266-3538(03)00096-4

[10] Ilyas, R. A., Sapuan, S. M., Harussani, M. M., Hakimi, M. Y. A. Y., Haziq, M. Z. M., Atikah, M. S. N., Asyraf, M. R. M., Ishak, M. R., Razman, M. R., Nurazzi, N. M., Norrrahim, M. N. F., Abral, H., & Asrofi, M. (2021). Polylactic Acid (PLA) Biocomposite: Processing, Additive Manufacturing and Advanced Applications. Polymers, 13(8), 1326. https://doi.org/10.3390/polym13081326

[11] Ku, H., Wang, H., Pattarachaiyakoop, N., & Trada, M. (2011). A review on the tensile properties of natural fiber reinforced polymer composites. Composites Part B Engineering, 42(4), 856–873. https://doi.org/10.1016/j.compositesb.2011.01.010

[12] Asim, M., Paridah, M. T., Chandrasekar, M., Shahroze, R. M., Jawaid, M., Nasir, M., & Siakeng, R. (2020). Thermal stability of natural fibers and their polymer composites. Iranian Polymer Journal, 29(7), 625-648. https://doi.org/10.1007/s13726-020-00824-6

[13] Sanjay, M. R., Siengchin, S., Parameswaranpillai, J., Jawaid, M., Pruncu, C. I., & Khan, A. (2019). A comprehensive review of techniques for natural fibers as reinforcement in composites: Preparation, processing and characterization. Carbohydrate polymers, 207, 108-121. https://doi.org/10.1016/j.carbpol.2018.11.083

[14] Venkateshwaran, N., & Elayaperumal, A. (2010). Banana Fiber Reinforced Polymer Composites - a review. Journal of Reinforced Plastics and Composites, 29(15), 2387–2396. https://doi.org/10.1177/0731684409360578

[15] Parvin, S. (2014). Physico-mechanical properties of chemically treated jute fibre reinforced plastic composites

[16] Olubajo, O. O., Paul, A. S., Olubajo, O. O., & Paul, A. S. (2024). Strength prediction and optimisation of velvet tamarind pod ash cement blends via response surface methodology. Olubajo | Path of Science. https://doi.org/10.22178/pos.106-49

[17] Suhot, M. A., Hassan, M. Z., Aziz, S. A., & Md Daud, M. Y. (2021). Recent Progress of Rice Husk Reinforced Polymer Composites: A Review. Polymers, 13(15), 2391. https://doi.org/10.3390/polym13152391

[18] Horrocks, A. R. (2008). Flame retardant/resistant textile coatings and laminates. In Advances in fire retardant materials (pp. 159-187). Woodhead Publishing. https://doi.org/10.1533/9781845694701.1.159

[19] Devireddy, S. B. R. (2017). Mechanical, thermal and physical properties of hybrid banana-jute fibers reinforced epoxy and polyester composites: modeling and experiments (Doctoral dissertation.

[20] Oyejobi, D. O., Raji, S. A., Aina, S. T., & Siva, A. (2019). Physio-chemical and microstructural characteristics of selected pozzolanic materials for cement and concrete production. Nigerian Journal of Technological Development, 16(3), 111-119.

[21] Mohanty, A. K., Misra, M., & Drzal, L. T. (Eds.). (2005). Natural fibers, biopolymers, and biocomposites. CRC press.

[22] Pickering, K. L., Efendy, M. A., & Le, T. M. (2016). A review of recent developments in natural fibre composites and their mechanical performance. Composites Part A: Applied Science and Manufacturing, 83, 98-112. https://doi.org/10.1016/j.compositesa.2015.08.038

[23] Daramola, O. O., Akinwande, A. A., Adediran, A. A., Balogun, O. A., Olajide, J. L., Adedoyin, K. J., Adewuyi, B. O., & Jen, T. C. (2023). Optimization of the mechanical properties of polyester/coconut shell ash (CSA) composite for light-weight engineering applications. Scientific Reports, 13(1), 1066. https://doi.org/10.1038/s41598-022-26632-x

[24] Venkateshwaran, N., & Elayaperumal, A. (2010b). Banana Fiber Reinforced Polymer Composites - a review. Journal of Reinforced Plastics Composites, 29(15), 2387–2396. https://doi.org/10.1177/0731684409360578